Synthesis and in vivo behaviour of PVP/CMC/Agar hydrogel membranes impregnated with silver nanoparticles for wound healing applications

*Gabriel G. de Lima [1], Darlla W. F. de Lima [2], Maria J. A. de Oliveira [3], Ademar B. Lugão [3], Mara T. S. Alcântara [3], Declan M. Devine [1,4] Marcelo J. C. de Sá * [1,2]*

[1]Materials Research Institute, Athlone Institute of Technology, Athlone, Ireland.

[2]Veterinary Hospital, Patos Campus. Federal University of Campina Grande, Paraiba, Brazil.

[3]Laboratory of Biomaterials; Institute of Energy and Nuclear Research, São Paulo, Brazil.

[4]Rehabilitation Medicine Centre, Mayo Clinic, Rochester, MN, USA.

*Corresponding author - e-mail address: mjcdesa@research.ait.ie

ABSTRACT: The field of wound healing has seen an increase in research activity in wound care and hydrogels-based dressings have been targeted as a solution for these applications. Hydrogels with silver nanoparticles can present many advantages for this field. However, if the aggregation and sterilization of this product have not been carefully considered, the effectiveness or use could be limited. Therefore, in the current study, a hydrogel based wound dressing membrane was developed using polyvinylpyrrolidone (PVP), polyethylene glycol (PEG), agar and Carboxymethyl cellulose (CMC). Silver ions (Ag+) was dispersed in the polymer matrix and its reduction with formation of a hydrogel and silver nanoparticles was performed using 60Co gamma irradiation to enhance the dressings antimicrobial properties. The resulting hydrogel presented a high degree of swelling and a good size control of silver nanoparticles. The incorporation of AgNPs was confirmed via Raman spectroscopy and the samples presented no signs of toxicity in vitro as assessed using an elution assay with neutral red uptake as the cytotoxic endpoint. Membranes were tested in vivo using a full thickness

defeat model in rabbits. Post mortem histopathological analysis indicated that the use of the hydrogel membranes which incorporated AgNPs had a stimulatory action on wound healing as evidenced by a high intensity of fibroblasts and neovascularization in the tissue which promoted a faster healing process when compared to the untreated wounds. We demonstrate the possibility in producing a hydrogel with good size control of AgNPs which can also be directly sterilized within the formation of this material via gamma irradiation. Furthermore, the mechanism of hydrogel healing, *in vivo*, with silver nanoparticles was found to have a directly correlation of silver nanoparticles with in vitro cells results.

KEYWORDS Wound healing, silver nanoparticles, hydrogel, tissue engineering

INTRODUCTION

Skin is an important organ that protects the internal organs, muscles, bones and ligaments from the external environment. However, its protection can be decreased or lost as a result of injury and depending on the extent of the damage it can take several weeks or months to heal. If the wound is left untreated, the damaged skin is susceptible to invasion of microorganisms leading to a wound infection [1,2]. Hence much research has being undertaken for the development of wound healing dressings that can accelerate wound closure.

Ideally, materials for wound dressing must contain certain characteristics such as absorption ability of wound fluids and pus, act as a bacterial barrier, promote functional adhesion i.e. can adhere to healthy tissue but not adhere to wound tissue, as well as easy to remove with low cost [3,4].

Hydrogels can be a potential solution for wound dressings [5–7] since these materials can produce a moist environment and help regenerate the skin with no scar while also possessing great ventilation ability and efficiently absorbing contaminated exudates [8]. Although hydrogels are ideal candidates for wound dressing applications, most common and biocompatible hydrogels lack antibacterial properties, which help prevent infection. The incorporation of silver nanoparticles (AgNPs) not only

helps to prevent infections but these nanoparticles also have a growth-inhibitory capacity against microorganisms [9]; which unlike conventional chemical antimicrobial agents does not enable microorganism improve their drug resistance over generations [10].

AgNPs have unique properties such as their ability to cover a broad-spectrum of microorganisms with low toxicity and can be used in medicine or pharmaceutical fields [11,12]. However, AgNPs readily aggregate due to its strong dipole-dipole attraction and high surface energy. This aggregation leads to a loss in antibacterial activity [13,14]. For these reasons, various surfactants and polymers are used enhance dispersion of AgNPs. It has being proposed that hydrogels alleviate these issues by not only acting as a reservoir for a large quantity of AgNPs but can also address the dispersion problem [15]. Furthermore, the release of the nanoparticles in therapeutic doses plays a critical role in the healing parameter; which can also be optimized using hydrogels [16].

Polyvinylpyrrolidone (PVP) based hydrogels have been found to reduce AgNPs agglomeration as it can reduce the formation of Ag+ ions which, if found in higher quantity in the solution, could decrease the biocompatibility and can lead to toxic effects [17,18]. However, conventional methods of incorporating AgNPs into a polymer matrix cause easy lead to aggregation. Hence, an alternative approach is to use gamma-irradiation to aid dispersion. as this has been successfully used for preparation of nanometallic/polymer composites since the γ-ray irradiation can reduce the metallic ions to zero valiant metal particles [19].

Although, various wound silver dressings have been tested but there is insufficient evidence that silver nanoparticles actually promotes wound healing [20,21]. Available evidence that confirms the usefulness of silver is lacking [22]. The current study investigates a novel hydrogel which attempts to provide a better solution for improvement in the healing rates of wounds.

Several polymers have been shown to be suitable candidates for applications on wound dressings [8,23,24]. However, for these materials to have the capability of being used with these applications it is

necessary a proper sterilization as to not being contaminated. At the same time, the drug encapsulated onto the hydrogel, that can act as an anti-infective barrier, need to be well dispersed in the matrix [25]. In terms of silver nanoparticles an addendum requires its stabilization and good size control [21,26]. Further methods of sterilization by autoclave, the most used method in medical field, could not only disrupt the polymer matrix but at the same time reduce the dispersibility of AgNPs [27].

Although, PVP is well-established for their use on this field [28,29] mainly due to its biocompatibility; but PVP has inferior mechanical properties and low swelling capability limiting its potential [30]. For these reasons, this polymer is usually blended with polysaccharides to improve these desirable properties, while at the same time it can also improve its biodegradability and cytotoxicity [30]. The use of PVP/CMC and PVP/PEG/agar for wound dressings are already known to have great results and nowadays, these hydrogels are available in market under brand name 'Kikgel' and 'Aqua-gel' used for dressing of wound [31].

There is plenty of material which synthesize PVP/CMC in literature for wound healing but the actual application of its potential *in vitro* and *in vivo* are still lacking a thoroughly investigation, also when drugs are incorporated into this material, such as silver nanoparticles. In addition, the investigation on wound healing of PVP-CMC suffered a declined in the recent years being now explored towards bone regeneration [32,33].

Therefore, for this work a PVP based hydrogel was utilized. Polyethylene glycol (PEG) and agar were incorporated into the polymer structure to enhance the mechanical properties of the hydrogel. Additionally, Carboxymethyl cellulose (CMC) was added due to its high water solubility, low cost and high swelling capacity [34].

EXPERIMENTAL PROCEDURES

Materials. Poly(n-2-vinyl-pyrrolidone) (PVP)K90 (Basf,Brazil), Poly(ethylene glycol) (PEG 400) (Oxiteno,USA), Agar (Exodo, USA) and 22 ppm of colloidal Silver prepared by water electrolysis with silver electrodes (Khemia, Brazil) were used as received for hydrogels preparation. CMC-Na salt (Carboxymethyl cellulose sodium salt P.A). (Synth Brazil). Minimum Eagle's medium was obtained from Sigma Co (Brazil). The NCTC L929 cell line derived from mouse connective tissue was obtained from American Type Culture Collection (ATCC) tissue bank.

Hydrogel membranes preparation. Hydrogel membranes preparation. Hydrogels were prepared from mixture of PVP (8% w/v), CMC (0.5% w/v), Agar (1.0%) and PEG300 (1.5%) using the aqueous solution with Ag+ silver ions as the solvent yielding a final concentration of 11% of polymer and 89% silver solution in the mixture. Samples were incubated at 132 °C in an autoclave for 40 minutes to allow dissolution to take place. Hydrogel membranes were subsequently obtained by pouring the resulting solution on plastics supports with approximate dimensions of 80mm x 135mm and 2 mm thick. After cooling at room temperature, the hydrogels were covered by polyethylene film, sealed under inert atmosphere (N2) and irradiated with gamma rays from Cobalt 60 (60Co) at total dose of 25 kGy and dose rate of 10 kGy/h. This step allows the crosslinking of PVP/CMC that forms the hydrogel, and also reduces the silver ions forming the nanoparticles, stability and sterilization occur simultaneously by ionizing irradiation. The particle size is about 50 nm. The final composite hydrogel membranes were designated as PVP+PEG+agar for samples containing only PVP, PEG and agar; PVP+CMC for samples containing PVP, PEG, agar and CMC; PVP+AgNPs for samples containing PVP, PEG, agar and AgNPs and finally PVP+CMC+AgNPs for samples containing PVP, PEG, CMC, agar and AgNPs.

Transmission Electron Microscopy. To confirm the presence of silver nanoparticles in the hydrogel, a 2 x2 cm sample was placed in an Erlenmeyer and 20 mL of milli-Q water was added under stirring for 24 hours to promote the release of the silver nanoparticles. Subsequently, a drop of the

solution was placed on a carbon grid and analysed using a JOEL 2100 Electronic Transmission Electron Microscope (TEM).

Visible UV spectroscopy.

Visible UV spectroscopy was performed at wavelengths from 300 to 700 nm to confirm the presence of AgNPs in the prepared hydrogels , using SpectroMax® i3 Molecular Devices equipment.

Swelling.

Irradiated samples were freeze-dried. Dried samples were immersing in pH 7 buffer solution at 25 ºC in triplicate. At predetermined time intervals of up to 48h samples were removed from the buffer and weighed. The swelling was calculated using equation (1) .

Swelling = (ms - md)/md x 100 (1)

where: ms is the mass of swollen and md is the mass of dry hydrogel.

Silver nanoparticles release.

Hydrogel samples were placed into a flask containing 40mL of buffer pH 7.4. Samples were incubated at 37.0 ° C under shaking at 120 rpm. At time intervals of 1, 3, 7, 9, 24 and 48h, 2 ml aliquots were withdrawn from each flask and replaced with 2 ml of fresh buffer. The rate of AgNP release was measured using a Varian AA220-FS Atomic Absorption Spectrometer measured at 328 nm.

Raman confocal Microscopy and Dark Field Microscopy.

Cross section slices of 1 mm were analysed in Alpha300R confocal Raman (WiTec) microscope using 100x lenses, 532 nm wavelength laser and 10mW potency. Hyperspectral dark-field images were obtained by placing hydrogel samples between two glass laminas (2 mm and 0.1 mm thickness), under white light and 100x objective lenses in a Dark Field Hyperspectral microscope (Cytoviva, Auburn, AL).

Particle size analysis - Dynamic light scattering (DLS).

A dynamic light scattering method was used to determine AgNPs size using a Brookhaven Instruments Corporation DLS. The particle size (multimodal size distribution) was determined by measuring the angles at which an incident light beam is scattered as a function of the Brownian motion of the colloidal silver particles. Standard setting of 35 mW red diode laser and nominal 640 nm wavelength were utilised.

For DLS analysis, pure AgNPs were measured by heating 22 ppm silver ions solution and then irradiated. The silver nanoparticles in the PVP and PVP+CMC hydrogels were extracted in aqueous solution under sonication for 24h prior to testing.

Cytotoxicity.

The methodology for cytotoxicity was based on [35] which is specific for test toxicity of biocompatible polymers which is a slightly modified version of [36].

Test samples were immersed in minimum Eagle's medium (Sigma Co., Brazil) for 24h at 37ºC. Serial dilutions of the extracts were incubated with NCTC L929 cell line, cultured on 96 wells microplate.

Cytotoxicity tests were evaluated by Neutral red uptake assay, measured in spectrophotometer with 540 nm at the end of the assay.

Negative and positive controls are used to determine the reference limits of the results. The negative control (no toxic compound) used was high density polyethylene (HDPE) and positive control was natural rubber latex film, which has a toxic effect on cells.

The cell viability percentage was plotted against extract concentration and the final graphic corresponds to the viability curves of each sample and controls. Sample with viability curve above 50% cell viability line is considered non-cytotoxic.

In Vivo experimentation

The research project was evaluated and approved by the Research Ethics Committee of the Federal University of Campina Grande (UFCG) number 002/2006. Ten New Zealand white rabbits with an average weight of 2kg were used in this study. They were maintained in a temperature – regulated environment (24°C) on a 12 h light/dark cycle. The animals were housed individually in rabbit cages under the same feeding and management conditions. The animals were acclimatized for 15 days prior to the experiments.

Prior to surgery the animals received neurolept analgesia with acepromazine 0.2 mg/kg associated to tramadol 2mg/kg intramuscularly. EMLA® (AstraZeneca LTDA, São Paulo, Brazil) was used topically 30 min before the surgery procedure for viability of the local blocking, this blocked was achieved with lidocaine 2% (9mg/kg), 1.5 ml/site of incision. Anti-inflammatory meloxicam was used via SC 0.2 mg/kg. In addition, antibiotic therapy was performed via intravenously with enrofloxacin 5 mg/kg. The animals also had trichotomy in dorsal region, the antiseptic of skin was performed with chlorhexidine 0.5% in the surgery location. The surgery was performed using a scalpel, making incisions in the skins of the animals with the help of a caliper with 1.5 cm^2 of area. These incisions were followed by divulsion of the subcutaneous and exposure of muscular fascia in the animal dorsal thoracic region, between T4(fourth thoracic vertebra) and T13 (13th thoracic vertebra), where it was further removed two fragments of skin with 1.5 cm2 area (Figure 1) which was approximately 5 cm of length between each surgery wound.

After removal of the two fragments, the animals were divided by random, to compose the experimental groups. Named as Biofilm-2 (GB-2) for the wounds that received the hydrogel membrane that were changed after each 2 days and for the group that the hydrogel was changed after 4 days was named as Biofilm-4 (GB-4). The untreated wound was named as Control Group (GC). Finally, the wounds were covered with sterile gauze, microporous surgical tape and compressive bandage. Daily care on the site of the wounds was performed in all subjects. The dressing materials

were changed according to the experimental group. The experimental endpoints for these groups were days 7, 14, 19, 21, 23 and 25 to evaluate the dimension of the wounds in all experimental groups until complete regression of the wound on all groups.

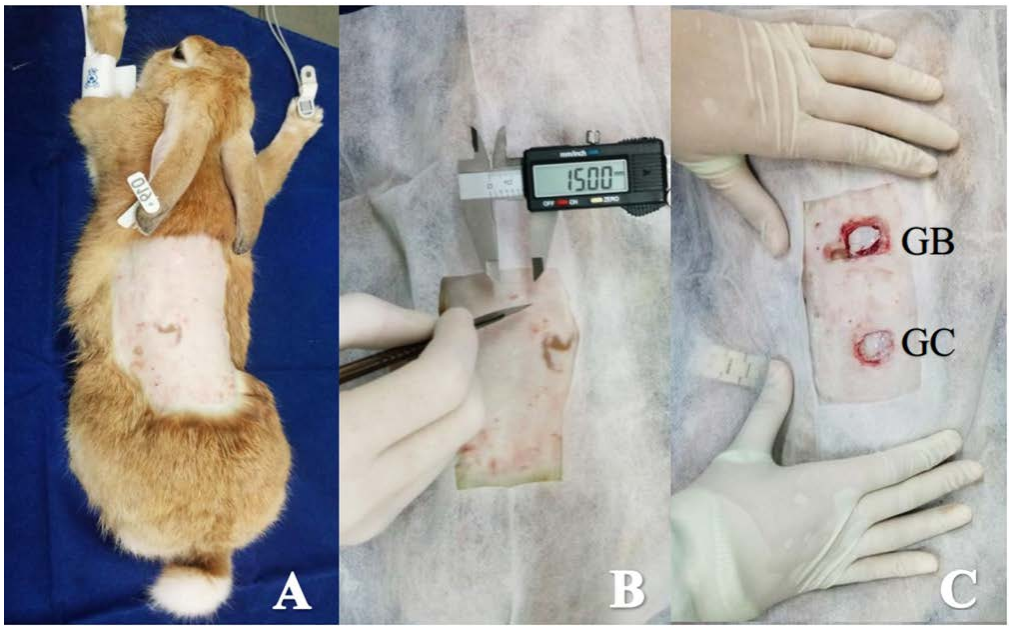

Figure 1 - (A) Immediate preoperative, surgical field after trichotomy. (B) Measurement of the size of the surgical lesions with digital caliper. (C) Removal of cutaneous fragment with 1.5 cm^2 extension in the back region of the animal.

Microscopic analysis were conducted and compared with the control group and group GB2. The experimental endpoints of microscopy analysis were days 3,7 and 14.Post mortem of the area comprising the wound was removed for histological analysis. The samples were fixed in formalin solution. Afterwards, the samples were embedded with paraffin and sectioned longitudinally in 5 µm thick sections, the sections were surface stained with haematoxylin and eosin. The stained sections were analysed under a light microscope considering the following data: level of inflammation, fibroblasts and neo-vascularisation. These cells were counted via glass slide dividing it by ten different fields, in each of these fields the number of cells was gathered individually, and the mean value was

used for statistical analysis. The number of epidermis layers were counted on the wound and compared with health skin tissue.

Statistical analysis.

Statistical analysis was performed with Graph pad Instat software. A comparison between the experimental parameters within each group was performed using analysis of variance for repeated samples, followed by the non-parametric Friedman test. For comparison between groups, at each experimental moment the parametric Student's t-test was used for independent samples. Both tests were applied at the 5% level of significance.

RESULTS

Silver Nanoparticles Solution

AgNPs were formed following autoclaving and irradiation of silver solutions. Fig. 2 shows the evolution of AgNPs formation from transparent ionic silver solution (A); to the initial stages of AgNPs formation after autoclaving (B) and the final intense brown colour evidenced by the AgNPs formation after autoclaving and irradiation (C), which can be verified by the UV-Vis spectra (D).

Usually, in silver nanoparticles, the conduction band and valence band lie very close to each other in which electrons move freely. These free electrons give rise to a surface plasmon resonance (SPR) absorption band (380–500 nm range) due to the collective oscillation of electrons of silver nanoparticles in resonance with the light wave of UV-Vis spectroscopy [37]. A significant improvement in the absorption peak (λmax = 420 nm) was observed due to the SPR effect as seen in Fig.2 (D).

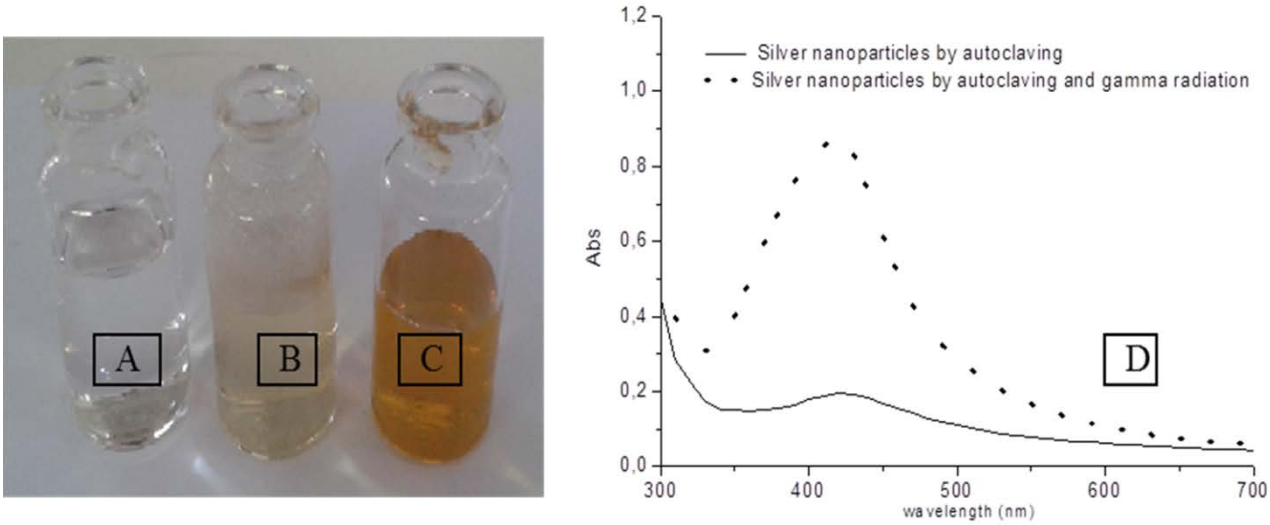

Figure 2 - Solution containing silver ions (A); after autoclave(B); after autoclave and irradiation (C) and UV-Vis spectra of AgNPs (D).

Dynamic light scattering

In Fig. 3 the DLS multimodal size distribution histograms correspond to (A) AgNPs solution, (B) AgNPs released from PVP hydrogel and (C) AgNPs released from PVP+CMC hydrogel. The silver nanoparticles appear to indicate slightly varied groups of aggregates with different mean diameters.

As expected, the pure silver nanoparticles presented a large particle size and standard deviation (Figure 3) while the addition of PVP largely reduces these values; the further addition of CMC affects the silver nanoparticles sizes since it exhibits a small standard deviation with a particle size mean of 31 nm.

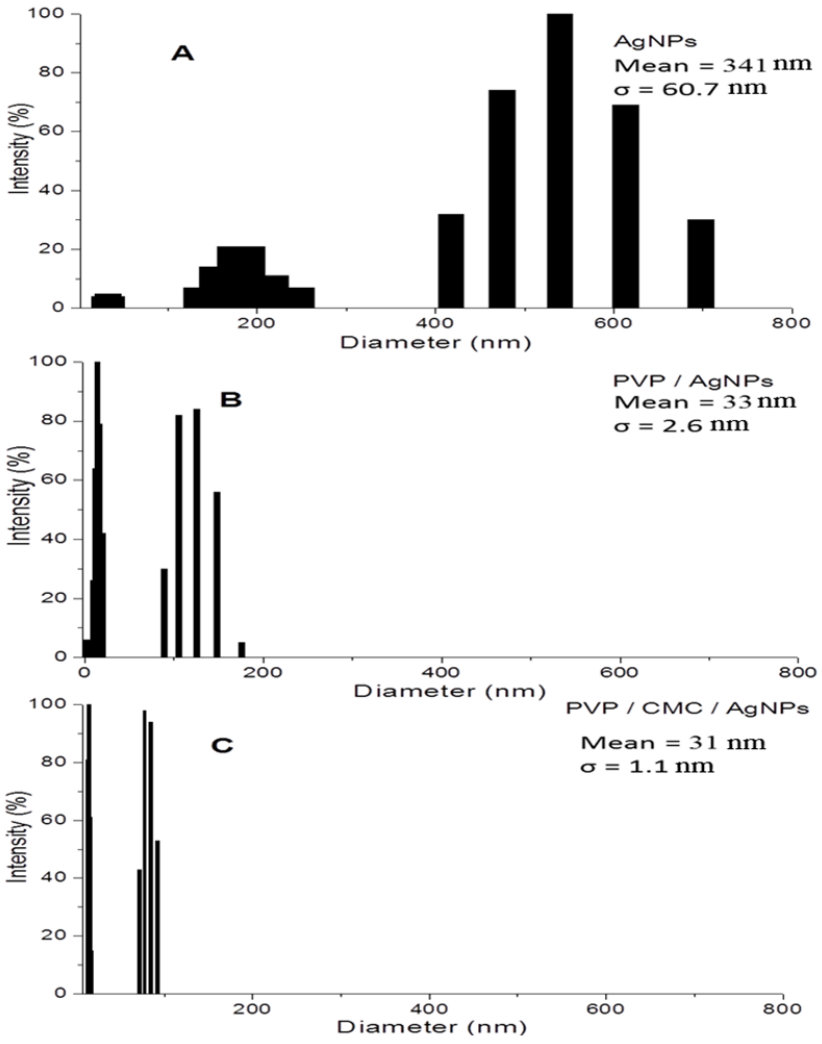

Figure 3 - Silver nanoparticles size distribution: (A) AgNPs solution 22 ppm, (B) AgNPs released from PVP+AgNPs hydrogel, (C) AgNPs released from PVP+CMC+AgNPs hydrogel

Morphology Inspection

TEM confirms the formation of Ag nanoparticles (Fig.4) which exhibit a monodisperse structure with spheroidal shape and, in the specific sample analysed on TEM, PVP+CMC+AgNPs average diameter with standard deviation of 21 ± 4 nm which closely matches values obtained from DLS measurements.

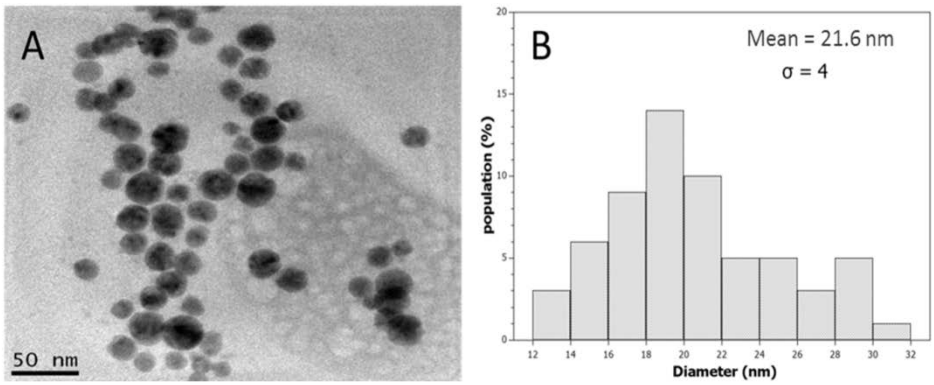

Figure 4 - (A) TEM of PVP+CMC and (B) size AgNPs distribution histogram

Swelling and AgNP release

The presence of AgNPs in the hydrogel has little effect on the swelling behaviour of the hydrogels produced with PVP (Fig.5). However, the addition of small amounts of CMC, increases the swelling from ~ 100% to values higher than 400%. Crosslink density is noticeably one of the most important factor concerning the swelling, followed by the presence of functional groups [38,39]. In this study chemical crosslinking was a result of recombination of free radicals generated by irradiation [40].

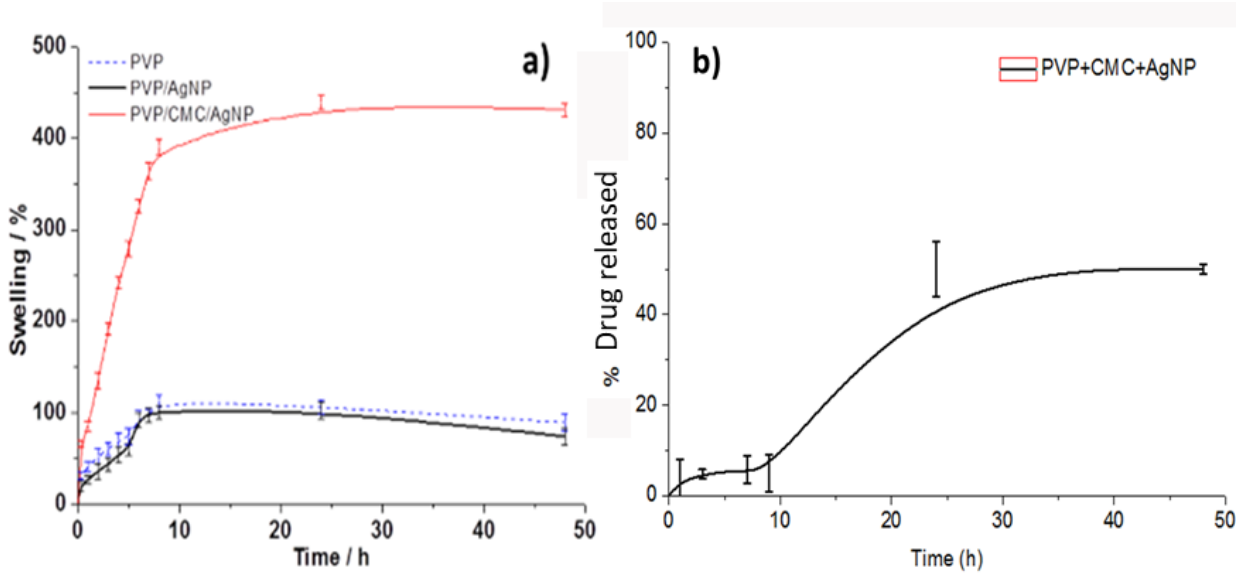

Figure 5 - a) Swelling ratio of PVP, PVP+AgNPs and PVP+CMC+AgNPs. b) AgNP release profiles of PVP+CMC+AgNPs.

The release profiles for AgNPs from the PVP+CMC samples exhibited an initial burst release up to the 3 h time point with relative stability of release thereafter up to 40 h after which the release plateaued.

Microstructure profile

Raman and dark field hyperspectral images obtained from PVP+CMC hydrogel with AgNPs confirm the presence of AgNPs which presented as illuminated spots in the photomicrograph (Fig.6a-b) and as new peaks in the Raman spectrum between 1500 and 1800 cm^{-1} (Fig.6c), when compared to the hydrogel without AgNPs. These peaks are characteristic for silver particles and their presence suggests formation of AgNPs.

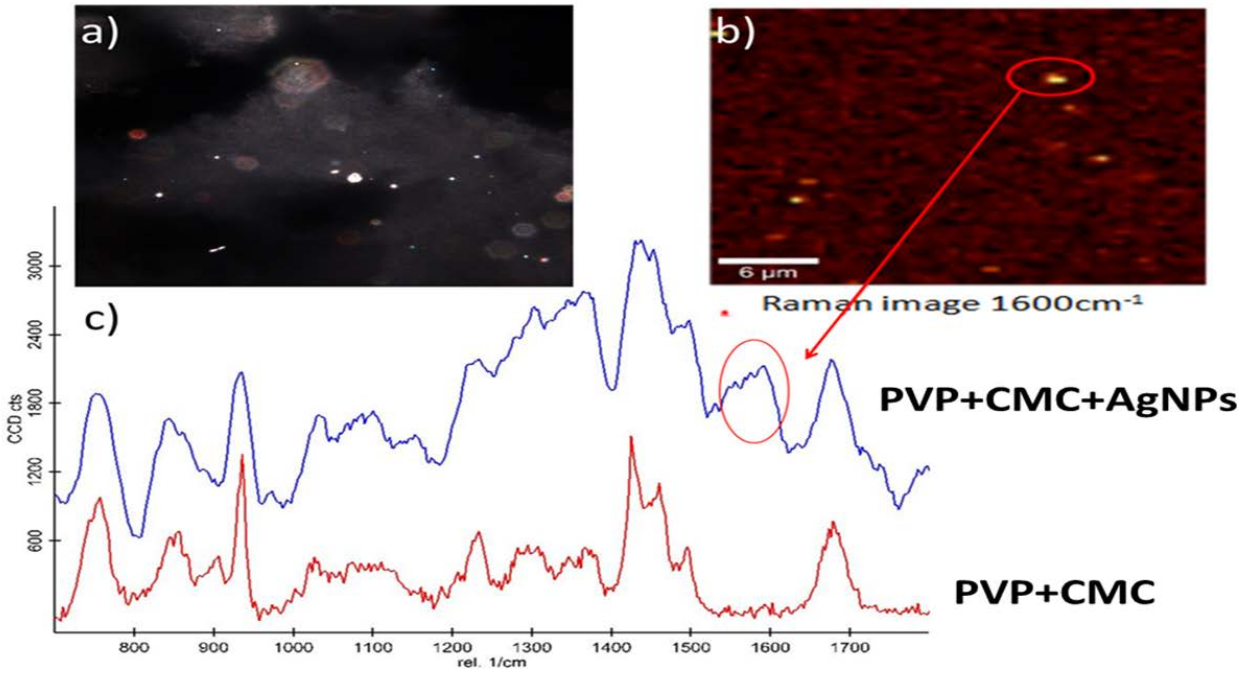

Figure 6 - (a) Dark field hyperspectral images of AgNPs in PVP+CMC hydrogels, (b) AgNPs in confocal microscope and (c) Raman image of silver particles (red) and polymeric membrane (PVP+CMC+AgNPs (blue)

Cytotoxicity

Cytotoxicity tests exhibit identical behaviour for the test sample and that of the negative control (Fig.7). Therefore, it is possible to state that the elations from the hydrogels synthetized by gamma crosslinking, in this study, do not harm the mammalian cell; they can thus be characterized as non-cytotoxic. Positive controls as expected did cause a cytotoxic response lower than 50% cell viability.

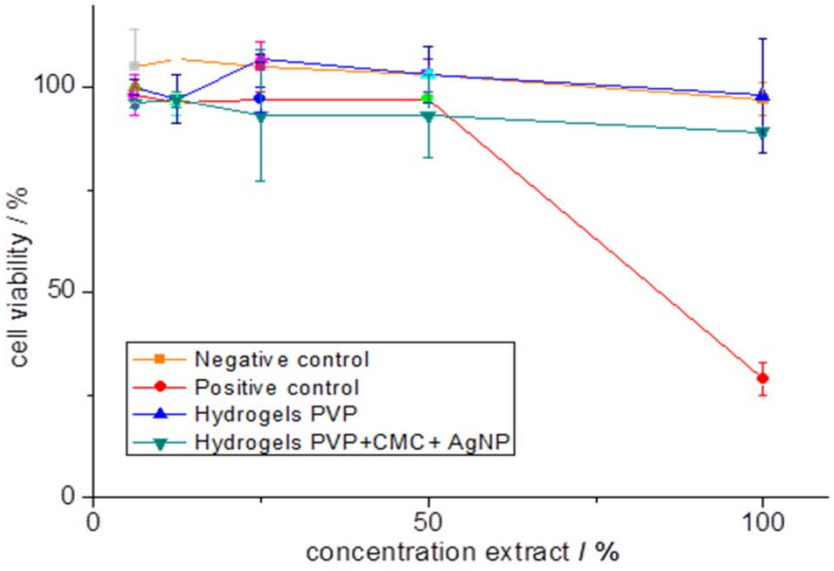

Figure 7 - Cell viability curves based on the neutral red cytotoxicity assay which illustrated the cytocompatibility of the hydrogel membranes tested.

In vivo Macroscopic evaluation

The healing process of the experimental wounds is shown in Figure 8. The animals studied in this work had a good recovery from the surgeries with no signs of infection. During the trans- and post-operative period, no aseptic failure or surgical problems that could compromises the results of the experiment occurred. In addition, the animals also exhibited a healthy status in the post-operative period. This strongly suggest the effect of AgNPs which indicates that these nanoparticles have immediate and residual antimicrobial effect which assists in the process of wound healing of the skin by reducing the risks of infection in the wound, as reported by several other authors [16,19] .The local

exudates results indicates that after the first change of bandages, it was observed a large quantity of serum absorbed by the compressed gauze, positioned between the wound of the untreated group. By removing the compressed gauze, the wound of CG presented a dried aspect while the GT exhibited a humid environment between the hydrogel membrane and the wound (figure 8a-b).

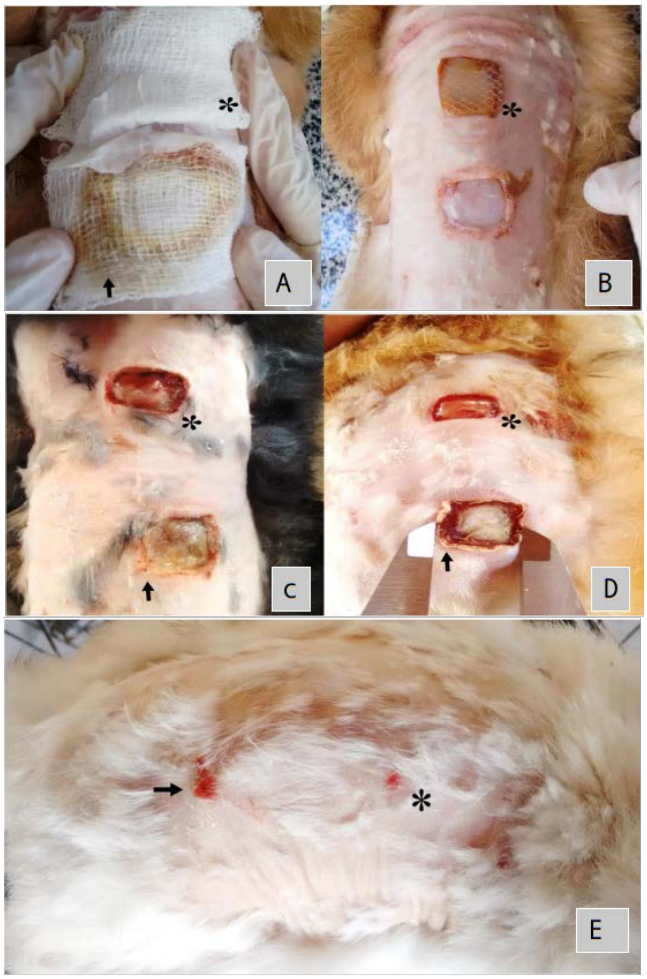

Figure 8 - GB4 at 4 days during first dressing exchange. (A) Presence of exudates absorbed by the dressing on the GC (arrow) when compared to GT (*). (B) After removal of the first dressing (*) GT. (C) GB4 at seven days - GT (*) and GC (arrow). (D) GB2 at seven days GT (*) and GC (arrow). (E) GB4 at 21 days, GT (*) and CG (arrow).

The scabbing formation that naturally protect the wounds exhibited an increase between the untreated wound compared to the treated groups. However, no differences were observed between the treated

groups of two and four days – GB2 and GB4. Additionally, granulated tissue were observed in higher quantity, with a more vivid red colour in the treated groups when compared to the control group and a visual difference of the same effect was observed in GB2 when compared to GB4 (Figure 8c-d).Regarding the wound size, treated wounds presented a fast reduction ratio when compared to the untreated wound (Figure 8e-9a) with no significant differences between the GB2 and GB4 in day seven of the experiment. The contraction and consequent closure of the wound occurred faster in GB2 when compared to GB4 in the final stages of wound healing. Finally, no visual differences and side-effects were perceived in local inflammation in between the studied groups.

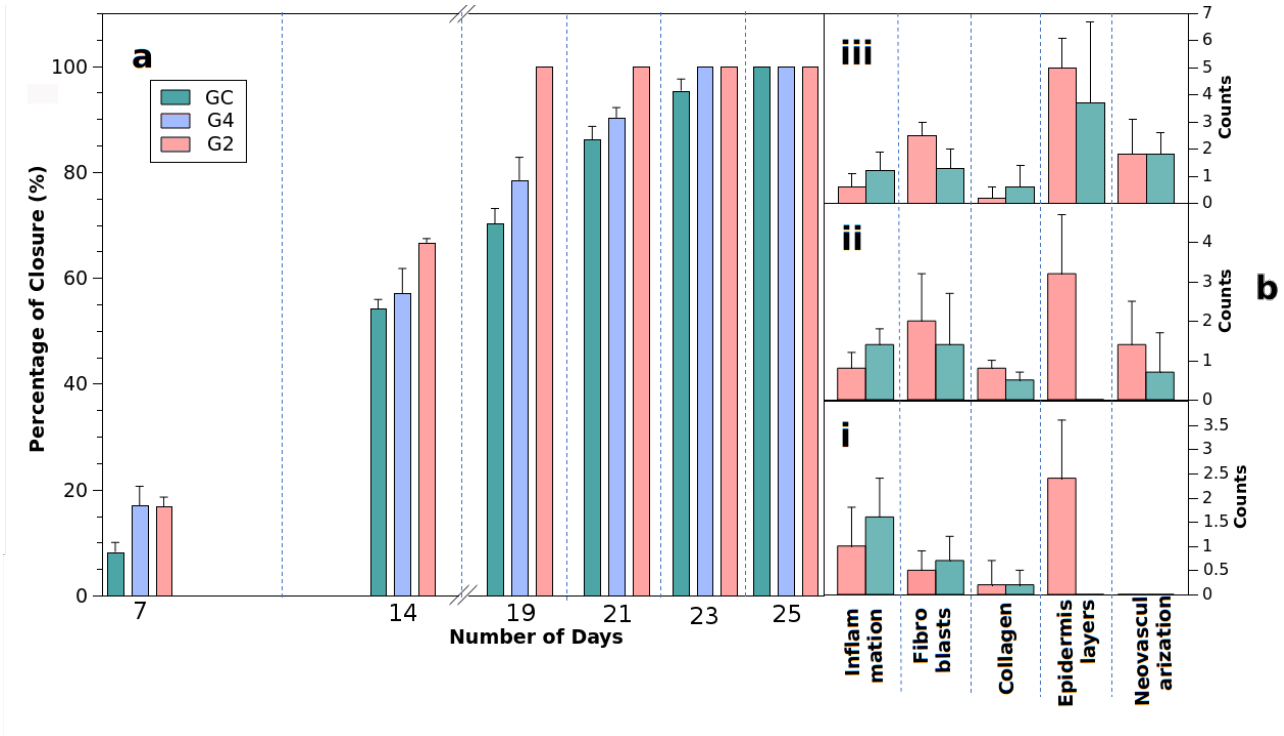

Figure 9 - Results for (a) macroscopic and (b) microscopic analysis of the wounds in the evaluation period of (i) three days, (ii) seven days and (iii) fourteen days.

In Vivo Microscopic analysis

The number of fibroblasts after 11 days for the hydrogel membrane increased significantly compared to 3 days in the PVP+CMC+AgNPs (p value <0.03) group and was significantly higher compared to the untreated wound (Figure 9b-10a-b). Neovascularization increased significantly after 11 days compared to 3 days in both groups (Figure 8b-9c-d).The number of epidermis layers in the untreated wound was significantly higher after seven days compared to three days. At the three-day time-point the hydrogel membrane had significantly increased epidermis (p value <0.03) layers compared to the untreated wound. All the other comparisons were non-significant (Figure 9b).

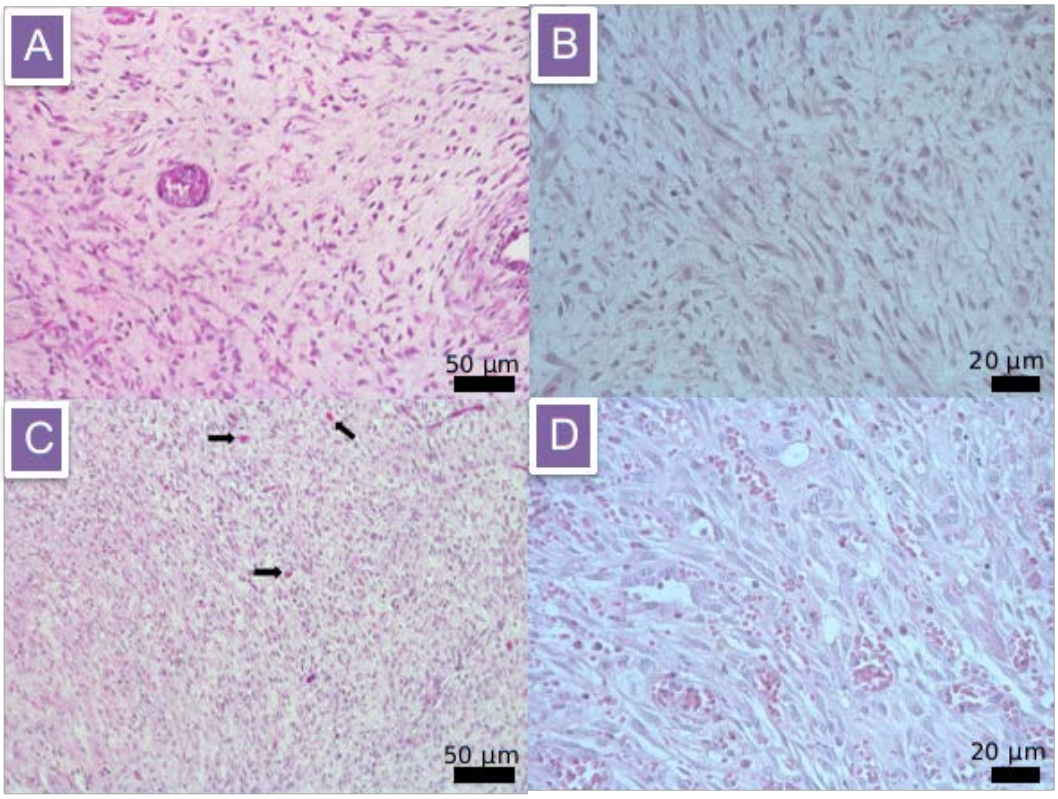

Figure 10. Photomicrograph of haematoxylin-eosin stained histology of sections at 14 postoperative days, with a 20x and 50x magnification, showing the amount of fibroblasts (small dark spots on the slide) for untreated (a) and treated (b) wound; the intensity of neoformed vessels (arrows) for untreated (c) and treated (d) wound.

DISCUSSION

PVP based hydrogels have being utilized for a variety of biomedical applications however, PVP is frequently used in conjunction with other polymers to improve its undesirable properties [40–42]. The incorporation PEG into the PVP system acts as a plasticizer to adjust the gelation and the maximum swelling of the hydrogel, while CMC and PEG both act as reducing agents and stabilizer for AgNPs [43,44]. In addition, the incorporating agar can improve the mechanical properties of the final gel [45]. The agar was used prior gelation of the PVP in the package, so it can facilitate handling until crosslinking occurred. The use of PEG for this hydrogel 1 to 2% as a plasticizer is sufficient to promote the mobility of the chains and make the hydrogel flexible.

These conditions were selected for optimal wound dressing application with the main focus of this work to investigate the *in vivo* behaviour of these hydrogels with special attention to the inflammatory reaction of the membranes in the in vivo environment. The hydrogel membrane produced in this work forms a protective gel cover of limited absorptive capacity and can be considered an interactive dressing as it can hydrate the wound and facilitate autolytic debridement. Furthermore, the selected hydrogel membrane was able to maintain hydrated state even after three days due to diffusion mechanism that controls this process [46].

To avoid the aggregation of AgNPs, the preparation of colloidal systems is usually carried out in the presence of species called stabilizers, which adsorb on the surfaces of the nanoparticles, forming a self-organized layer that prevents adhesion. To this end, some of the most effective stabilizers are those polymeric, such as, for example, polyvinylpyrrolidone (PVP) having in their structures basic Lewis sites with high affinity for the nanoparticles and long enough organic chains which create a steric hindrance, avoiding interactions between them.

The AgNPs solution presented a broader peak of SPR in UV-Vis spectra, which is characteristic of the broader size distribution. After gamma irradiation, there is an increase in SPR peak indicating an increase in the quantity of AgNPs and hence indicates an increase in intercalation of the AgNPs. The

decrease in the particle size is beneficial since the particle size plays an important role in the applications of AgNPs as their efficiency depends on its size.

There is a variation on the particle size, as exhibited on DLS, and the AgNPs have at least three groups leading to a large mean diameter and standard deviation which is a common behaviour depending on the process of formation of these nanoparticles [47]. When the AgNPs were incorporated into the hydrogel, only two groups were detected by the DLS and exhibited a more continuous dimension – very small mean diameter and standard deviation compared to pure AgNPs. The addition of CMC not only can help the mechanical properties of the hydrogel but it also can stabilize metallic nanoparticles [15]. These results are in agreement with DLS result which showed a more concise diameter and smaller standard deviation. It is surmised that the gamma irradiation, which produces a 3D polymeric matrix have inter-and intra- molecular bonding with radical linkage which inhibits the aggregation of AgNPs forming nanoparticles of smaller sizes [48].

Furthermore, the nanoparticles exhibited uniform structure with little aggregation based on TEM results; this lower aggregation might have happened since these polymers are known to stabilize the AgNPs [49]. However, the results obtained from TEM are the core size of particles and usually gives smaller results for coated particles than the ones obtained by DLS [50]. The size of PVP-coated AgNPs are correlated with apoptosis and decrease of cell viability [51], if the size of AgNPs are too small they tend to have a higher activity due to surface area regulating oxidation stress and its dissolution into ions [52,53].

Swelling results shows that there is no variation when adding AgNPs into the hydrogel structure. However, the incorporation of CMC increases the swelling by up 400%. This can be explained by two factors, one is the high hydrophilicity of CMC [54] and the second is that any chain network of polyelectrolyte with ionisable groups induces the mobile counter-ions presented into the hydrogel to develop a large swelling pressure due to intermolecular noncovalent interaction which, in this case, is

hydrogen-bonding [55]. This resulted in an increase in the swelling capability with the incorporation of CMC [56]. The AgNPs release profiles for the PVP hydrogels with CMC resembled that of other groups where a burst release was observed initially, followed by relatively stable release profile up to 40 h [57]. The release mechanisms of AgNPs in PVP hydrogels is controlled by the interdiffusion of the ions within the hydrogel.

Dark field hyperspectral images exhibit a well disperse AgNPs into the hydrogel membrane and the Raman results show in the spectra two new intense bands formed at 1600 cm^{-1} and 1800 cm^{-1}, confirming the incorporation of the AgNPs into the hydrogel. The peak at 1605 cm^{-1} is attributed to the carbonyl stretch group which is formed via the coordination between Ag+ and O, helping form a link between Ag+ and N atom on the pyrrolidone ring [58]. Borodko et al (2006) illustrates that metallic nanoparticles might link with PVP via the pyrrolidine rings and its assigned bands consists of the ones we obtained in this work [59].

Cytotoxicity tests exhibit no negative reactions through the cells and the hydrogel membrane followed the pattern of the negative control. The hydrogel membrane since it contained PVP+CMC results in a highly biocompatible material. The AgNPs incorporated into the hydrogel might have lowered the numbers of silver ions in the structure making the nanoparticles cytocompatible [60,61].

The macroscopic analysis of the wound on in vivo procedures revealed that the hydrogel membrane promotes a hydrophilic environment by inducing liberation of signalling that can stimulate the tissue regeneration [62]. In addition, increased formation of scabbing was observed in the untreated wound compared to when the hydrogel membrane was used. The prevention of scab formation helps promote the epithelization of experimental superficial wounds [23] and the smaller amount of scab observed in the hydrogel membrane might be due to the hydrophilic properties of the hydrogel, which increases the absorption of liquid from the wound, while also softening and removing the devitalized tissue helping angiogenesis and accelerating the tissue granulation process [63].

Regarding the hydrogel membranes, no significant differences were perceived in the amount of scabbing if periodically changed from two to four days (GB2 and GB4). The reduced scabbing formed by the hydrogel is an interesting factor because it can promote a better oxygenation since cells in regeneration greatly reduces the need to secrete enzymes to dissolve the scab and the cicatrisation formed is visually more aesthetic pleased. In addition, an increase in granulated tissue and reduction of the wound size with the treated hydrogel which are related to the hydrogel membrane since when changing at each two or four days in the initial stages of regeneration might promote an improvement in the upcoming macrophages cells in the local of the wound, with consequent proliferation and activation of fibroblasts forming the granulated tissue. The consequent closure of the wounds occurred faster in GB2 compared to GB4 in the final stages of cicatrisation. These observations were possible because in the final stages, when changing the hydrogel at each two days, is capable of promoting increased quantity of myofibroblasts and increased contraction of the borders of the wound. There was a visual improvement in cicatrisation of the wound with the hydrogel membrane, our hypothesis is that in the beginning of the wound healing there was little scab formation as the hydrogel membrane creates a humid environment in the region of the wound, which led to a targeted delivery of the AgNPs. This led to an increase in tissue neoformation, even if not statistically significant.

In vivo microscopic analysis shows that inflammation exhibited low values, and the treated wound had further reduced it indicating the healing properties of these membranes with the aid of AgNPs. The large number of fibroblasts indicates that the hydrogel stimulated the migration phase of the tissue healing [64]. Even though large quantity of fibroblasts was detected, the amount of collagen remained the same within the time of the study. Indeed the last time period for the hydrogel membranes revealed a decrease, although not significant, and this have been reported by researchers that AgNPs could reduce the formation of collagen by fibroblasts by driving their differentiation into myofibroblasts [65]. Myofibroblasts contracts the wound via intracellular contraction during the wound healing. This

behaviour can further be compared to the macroscopic images of the wound where 21 days the wound is more compacted than the untreated wound. This process occurs faster than re-epithelization because no cell proliferation is involved. The re-epithelization occurred with greater intensity in the hydrogel membrane during all the periods observed, exhibiting an increased thickness of the neoformed epithelium, and the layer thickness formed was similar to the normal tissue. The layers formed a dense connective tissue with new dermal layer. According to Liu et al., the faster re-epithelization may be induced by the AgNPs where it can promote the migration of keratinocytes from the edge of the wound to the centre and further differentiate and maturate it. The underlying mechanism of this process seems to be attributed to the Notch signalling pathway [66].

The hydrogel membranes promoted intense neovascularization when compared to the untreated wound, which have great importance for cell migration and nutrition with consequent tissue healing, and formation of new epidermis which correlates to reports in the literature [62]. Furthermore, faster the re-epithelialization lowers the risk of developing wound infection with accelerates healing of the wound. This can further be compared by the fact that the AgNPs can promote neovascularization via the promotion of angiogenesis and VEGFR signalling [63].

The characteristics of the materials used in these membranes provided the maintenance of an environment favourable for wound healing

CONCLUSION

The hydrogel membrane produced in this work exhibited varying sizes of AgNPs with uniform sphere shape. When CMC was added in the structure, it increased the swelling ratio to up 400%, which was attributed to the stabilization and due to inter- and intra- molecular bonding with radical linkage. Raman results confirmed the incorporation of AgNPs by the presence of bonds formed via carbonyl stretch group. Furthermore, the hydrogels studied in this work presented no sign of toxicity.

In vivo results indicated that scab formation was lower in the wound treated with the hydrogel membrane, which also exhibited increased cicatrisation. The analysis of the cell proliferation in the wound identified different inflammatory cells, which were suppressed or increased due to the AgNPs. Furthermore, large quantity of fibroblasts was detected with little formation of collagen, which was attributed to the differentiation into myofibroblasts. Finally, intense formation of re-epithelization and neovascularization was observed.

Therefore, we demonstrate in this work that this process is extremely original since not only provides in just one step, the reduction of Ag+ leading to stabilization of nanosilver but also PVP hydrogel formation with terminal sterilization via gamma irradiation. Therefore, there are two optimized processes that guarantee reproducible nanoparticles, stable, level of gelation. In addition, the developed membrane presented a very fast wound regeneration associated with AgNPs but at the same time, we were able to identify the mechanisms of silver nanoparticles with cell regeneration which was also correlated with *in vitro* results.

ACKNOWLEDGMENTS

The authors would like to acknowledge financial support from Coordenação de Aperfeiçoamento de Pessoal de Nível Superior - Brasil (CAPES) - Finance Code 001, CNPq, Science Without Borders and Comissão Nacional de Energia Nuclear (CNEN). Silver solutions and AgNPs were donated by Khemia, the authors would like to thanks Dr. Pablo Vasquez (CTR-IPEN- CNEN/SP) for irradiation, Instituto de Química (IQ/USP) for microscopy (Raman and Dark Field) and Lab microscopic and microanalyses IPEN.

REFERENCES

(1) Sorg, H.; Tilkorn, D. J.; Hager, S.; Hauser, J.; Mirastschijski, U. Skin Wound Healing: An

Update on the Current Knowledge and Concepts. *Eur. Surg. Res.* **2017**, *58* (1–2), 81–94.

(2) Han, G.; Ceilley, R. Chronic Wound Healing: A Review of Current Management and Treatments. *Adv. Ther.* **2017**, *34* (3), 599–610.

(3) Murdock, M. H.; Badylak, S. F. Biomaterials-Based in Situ Tissue Engineering. *Curr. Opin. Biomed. Eng.* **2017**, *1*, 4.

(4) Vowden, K.; Vowden, P. Wound Dressings: Principles and Practice. *Surg.* **2017**, *35* (9), 489–494.

(5) de Lima, G. G.; Lyons, S.; Devine, D. M.; Nugent, M. J. D. Electrospinning of Hydrogels for Biomedical Applications. In *Hydrogels*; Springer, 2018; pp 219–258.

(6) Caló, E.; Ballamy, L.; Khutoryanskiy, V. V. Hydrogels in Wound Management. *Hydrogels Des. Synth. Appl. Drug Deliv. Regen. Med.* **2018**, 128.

(7) Zhao, X.; Wu, H.; Guo, B.; Dong, R.; Qiu, Y.; Ma, P. X. Antibacterial Anti-Oxidant Electroactive Injectable Hydrogel as Self-Healing Wound Dressing with Hemostasis and Adhesiveness for Cutaneous Wound Healing. *Biomaterials* **2017**, *122*, 34–47.

(8) Zhao, X.; Sun, X.; Yildirimer, L.; Lang, Q.; Lin, Z. Y. W.; Zheng, R.; Zhang, Y.; Cui, W.; Annabi, N.; Khademhosseini, A. Cell Infiltrative Hydrogel Fibrous Scaffolds for Accelerated Wound Healing. *Acta Biomater.* **2017**, *49*, 66–77.

(9) Gopinath, V.; Priyadarshini, S.; Loke, M. F.; Arunkumar, J.; Marsili, E.; MubarakAli, D.; Velusamy, P.; Vadivelu, J. Biogenic Synthesis, Characterization of Antibacterial Silver Nanoparticles and Its Cell Cytotoxicity. *Arab. J. Chem.* **2017**, *10* (8), 1107–1117.

(10) Patra, J. K.; Baek, K.-H. Antibacterial Activity and Synergistic Antibacterial Potential of

Biosynthesized Silver Nanoparticles against Foodborne Pathogenic Bacteria along with Its Anticandidal and Antioxidant Effects. *Front. Microbiol.* **2017**, *8*, 167.

(11) Kim, D.; Kwon, S.-J.; Wu, X.; Sauve, J.; Lee, I.; Nam, J.; Kim, J.; Dordick, J. S. Selective Killing of Pathogenic Bacteria by Antimicrobial Silver Nanoparticle—Cell Wall Binding Domain Conjugates. *ACS Appl. Mater. Interfaces* **2018**, *10* (16), 13317–13324.

(12) Guo, Q.; Zhao, Y.; Dai, X.; Zhang, T.; Yu, Y.; Zhang, X.; Li, C. Functional Silver Nanocomposites as Broad-Spectrum Antimicrobial and Biofilm-Disrupting Agents. *ACS Appl. Mater. Interfaces* **2017**, *9* (20), 16834–16847.o

(13) Cunha, M. N. M.; Felgueiras, H. P.; Gouveia, I.; Zille, A. Synergistically Enhanced Stability of Laccase Immobilized on Synthesized Silver Nanoparticles with Water-Soluble Polymers. *Colloids Surf., B* **2017**, *154*, 210–220.

(14) Afshinnia, K.; Sikder, M.; Cai, B.; Baalousha, M. Effect of Nanomaterial and Media Physicochemical Properties on Ag NM Aggregation Kinetics. *J. Colloid Interface Sci.* **2017**, *487*, 192–200.

(15) Prema, P.; Thangapandiyan, S.; Immanuel, G. CMC Stabilized Nano Silver Synthesis, Characterization and Its Antibacterial and Synergistic Effect with Broad Spectrum Antibiotics. *Carbohydr. Polym.* **2017**, *158*, 141–148.

(16) Mekkawy, A. I.; El-Mokhtar, M. A.; Nafady, N. A.; Yousef, N.; Hamad, M. A.; El-Shanawany, S. M.; Ibrahim, E. H.; Elsabahy, M. In Vitro and in Vivo Evaluation of Biologically Synthesized Silver Nanoparticles for Topical Applications: Effect of Surface Coating and Loading into Hydrogels. *Int. J. Nanomedicine* **2017**, *12*, 759.

(17) Haque, M. N.; Kwon, S.; Cho, D. Formation and Stability Study of Silver Nano-Particles in

Aqueous and Organic Medium. *Korean J. Chem. Eng.* **2017**, *34* (7), 2072–2078.

(18) Gong, X.; Ma, Y.; Lin, J.; He, X.; Long, Z.; Chen, Q.; Liu, H. Tuning the Formation Process of Silver Nanoparticles in a Plasma Electrochemical System by Additives. *J. Electrochem. Soc.* **2018**, *165* (11), E540–E545.

(19) Ali, I.; Akl, M. R.; Meligi, G. A.; Saleh, T. A. Silver Nanoparticles Embedded in Polystyrene-Polyvinyl Pyrrolidone Nanocomposites Using γ-Ray Irradiation: Physico-Chemical Properties. *Results Phys.* **2017**, *7*, 1319–1328.

(20) Rashaan, Z. M.; Krijnen, P.; Klamer, R. R. M.; Schipper, I. B.; Dekkers, O. M.; Breederveld, R. S. Nonsilver Treatment vs. Silver Sulfadiazine in Treatment of Partial-thickness Burn Wounds in Children: A Systematic Review and Meta-analysis. *Wound Repair Regen.* **2014**, *22* (4), 473–482.

(21) Ousey, K.; Roberts, C.; Leaper, D. Silver-Containing Dressings. In *Wound Healing Biomaterials*; Elsevier, 2016; pp 403–437.

(22) Lindberg, T.; Andersson, O.; Palm, M.; Fagerström, C. A Systematic Review and Meta-Analysis of Dressings Used for Wound Healing: The Efficiency of Honey Compared to Silver on Burns. *Contemp. Nurse* **2015**, *51* (2–3), 121–134.

(23) Mir, M.; Ali, M. N.; Barakullah, A.; Gulzar, A.; Arshad, M.; Fatima, S.; Asad, M. Synthetic Polymeric Biomaterials for Wound Healing: A Review. *Prog. Biomater.* **2018**, *7* (1), 1–21.

(24) Archana, D.; Singh, B. K.; Dutta, J.; Dutta, P. K. Chitosan-PVP-Nano Silver Oxide Wound Dressing: In Vitro and in Vivo Evaluation. *Int. J. Biol. Macromol.* **2015**, *73*, 49–57.

(25) Saghazadeh, S.; Rinoldi, C.; Schot, M.; Kashaf, S. S.; Sharifi, F.; Jalilian, E.; Nuutila, K.;

Giatsidis, G.; Mostafalu, P.; Derakhshandeh, H. Drug Delivery Systems and Materials for Wound Healing Applications. *Adv. Drug Deliv. Rev.* **2018**.

(26) Joksić, G.; Stašić, J.; Filipović, J.; Šobot, A. V.; Trtica, M. Size of Silver Nanoparticles Determines Proliferation Ability of Human Circulating Lymphocytes in Vitro. *Toxicol. Lett.* **2016**, *247*, 29–34.

(27) Tipnis, N. P.; Burgess, D. J. Sterilization of Implantable Polymer-Based Medical Devices: A Review. *Int. J. Pharm.* **2018**, *544* (2), 455–460.

(28) Himly, N.; Darwis, D.; Hardiningsih, L. Poly(n-Vinylpyrrolidone) Hydrogels: 2.Hydrogel Composites as Wound Dressing for Tropical Environment. *Radiat. Phys. Chem.* **1993**, *42* (4–6), 911–914.

(29) Higa, O. Z.; Rogero, S. O.; Machado, L. D. B.; Mathor, M. B.; Lugão, A. B. Biocompatibility Study for PVP Wound Dressing Obtained in Different Conditions. *Radiat. Phys. Chem.* **1999**, *55* (5–6), 705–707.

(30) Roy, N.; Saha, N.; Kitano, T.; Saha, P. Novel Hydrogels of PVP–CMC and Their Swelling Effect on Viscoelastic Properties. *J. Appl. Polym. Sci.* **2010**, *117* (3), 1703–1710.

(31) Mishra, S.; Rani, P.; Sen, G.; Dey, K. P. Preparation, Properties and Application of Hydrogels: A Review - Hydrogels: Recent Advances; Thakur, V. K., Thakur, M. K., Eds.; Springer Singapore: Singapore, 2018; pp 145–173.

(32) Čadež, V.; Saha, N.; Sikirić, M. D.; Sáha, P. Viscoelastic Behavior of Mineralized (CaCO3) Chitin Based PVP-CMC Hydrogel Scaffolds. In *AIP Conference Proceedings*; AIP Publishing, 2017; Vol. 1843, p 50009.

(33) Saha, N.; Shah, R.; Gupta, P.; Mandal, B. B.; Alexandrova, R.; Sikiric, M. D.; Saha, P. PVP-CMC Hydrogel: An Excellent Bioinspired and Biocompatible Scaffold for Osseointegration. *Mater. Sci. Eng. C* **2018**.

(34) Ciolacu, D. E.; Suflet, D. M. Cellulose-Based Hydrogels for Medical/Pharmaceutical Applications. In *Biomass as Renewable Raw Material to Obtain Bioproducts of High-Tech Value*; Elsevier, 2018; pp 401–439.

(35) Rogero, S. O.; Malmonge, S. M.; Lugão, A. B.; Ikeda, T. I.; Miyamaru, L.; Cruz, Á. S. Biocompatibility Study of Polymeric Biomaterials. *Artif. Organs* **2003**, *27* (5), 424–427.

(36) Ciapetti, G.; Granchi, D.; Verri, E.; Savarino, L.; Cavedagna, D.; Pizzoferrato, A. Application of a Combination of Neutral Red and Amido Black Staining for Rapid, Reliable Cytotoxicity Testing of Biomaterials. *Biomaterials* **1996**, *17* (13), 1259–1264.

(37) Zhang, F.; Braun, G. B.; Shi, Y.; Zhang, Y.; Sun, X.; Reich, N. O.; Zhao, D.; Stucky, G. Fabrication of Ag@ SiO2@ Y2O3: Er Nanostructures for Bioimaging: Tuning of the Upconversion Fluorescence with Silver Nanoparticles. *J. Am. Chem. Soc.* **2010**, *132* (9), 2850–2851.

(38) Thombare, N.; Mishra, S.; Siddiqui, M. Z.; Jha, U.; Singh, D.; Mahajan, G. R. Design and Development of Guar Gum Based Novel, Superabsorbent and Moisture Retaining Hydrogels for Agricultural Applications. *Carbohydr. Polym.* **2018**, *185*, 169–178.

(39) Benhalima, T.; Ferfera-Harrar, H.; Lerari, D. Optimization of Carboxymethyl Cellulose Hydrogels Beads Generated by an Anionic Surfactant Micelle Templating for Cationic Dye Uptake: Swelling, Sorption and Reusability Studies. *Int. J. Biol. Macromol.* **2017**, *105*, 1025–1042.

(40) Demeter, M.; Virgolici, M.; Vancea, C.; Scarisoreanu, A.; Kaya, M. G. A.; Meltzer, V. Network Structure Studies on γ –irradiated Collagen–PVP Superabsorbent Hydrogels. *Radiat. Phys. Chem.* **2017**, *131*, 51–59.

(41) Devine, D. M.; Higginbotham, C. L. Synthesis and Characterisation of Chemically Crosslinked N-Vinyl Pyrrolidinone (NVP) Based Hydrogels. *Eur. Polym. J.* **2005**, *41* (6), 1272–1279.

(42) Song, G.; Zhao, Z.; Peng, X.; He, C.; Weiss, R. A.; Wang, H. Rheological Behavior of Tough PVP-in Situ-PAAm Hydrogels Physically Cross-Linked by Cooperative Hydrogen Bonding. *Macromolecules* **2016**, *49* (21), 8265–8273.

(43) Ganguly, S.; Ray, D.; Das, P.; Maity, P. P.; Mondal, S.; Aswal, V. K.; Dhara, S.; Das, N. C. Mechanically Robust Dual Responsive Water Dispersible-Graphene Based Conductive Elastomeric Hydrogel for Tunable Pulsatile Drug Release. *Ultrason. Sonochem.* **2018**, *42*, 212–227.

(44) Virkutyte, J.; Varma, R. S. Green Synthesis of Metal Nanoparticles: Biodegradable Polymers and Enzymes in Stabilization and Surface Functionalization. *Chem. Sci.* **2011**, *2* (5), 837.

(45) Qian L. (2018) Cellulose-Based Composite Hydrogels: Preparation, Structures, and Applications. In: *Cellulose-Based Superabsorbent Hydrogels. Polymers and Polymeric Composites: A Reference Series.* Springer, Cham.

(46) Chaudhuri, B.; Mondal, B.; Ray, S. K.; Sarkar, S. C. A Novel Biocompatible Conducting Polyvinyl Alcohol (PVA)-Polyvinylpyrrolidone (PVP)-Hydroxyapatite (HAP) Composite Scaffolds for Probable Biological Application. *Colloids Surf., B* **2016**, *143*, 71–80.

(47) Qasim, M.; Udomluck, N.; Chang, J.; Park, H.; Kim, K. Antimicrobial Activity of Silver

Nanoparticles Encapsulated in Poly-N-Isopropylacrylamide-Based Polymeric Nanoparticles. *Int. J. Nanomedicine* **2018**, *13*, 235.

(48) Gélvez, A. P. C.; Farias, L. H. S.; Pereira, V. S.; da Silva, I. C. M.; Costa, A. C.; Dias, C. G. B. T.; Costa, R. M. R.; Da Silva, S. H. M.; Rodrigues, A. P. D. Biosynthesis, Characterization and Leishmanicidal Activity of a Biocomposite Containing AgNPs-PVP-Glucantime. *Nanomedicine* **2018**, *13* (4), 373–390.

(49) Kvitek, L.; Panáček, A.; Soukupova, J.; Kolář, M.; Večeřová, R.; Prucek, R.; Holecova, M.; Zbořil, R. Effect of Surfactants and Polymers on Stability and Antibacterial Activity of Silver Nanoparticles (NPs). *J. Phys. Chem. C* **2008**, *112* (15), 5825–5834.

(50) Tejamaya, M.; Römer, I.; Merrifield, R. C.; Lead, J. R. Stability of Citrate, PVP, and PEG Coated Silver Nanoparticles in Ecotoxicology Media. *Environ. Sci. Technol.* **2012**, *46* (13), 7011–7017.

(51) Li, L.; Sun, J.; Li, X.; Zhang, Y.; Wang, Z.; Wang, C.; Dai, J.; Wang, Q. Controllable Synthesis of Monodispersed Silver Nanoparticles as Standards for Quantitative Assessment of Their Cytotoxicity. *Biomaterials* **2012**, *33* (6), 1714–1721.

(52) Kittler, S.; Greulich, C.; Diendorf, J.; Koller, M.; Epple, M. Toxicity of Silver Nanoparticles Increases during Storage Because of Slow Dissolution under Release of Silver Ions. *Chem. Mater.* **2010**, *22* (16), 4548–4554.

(53) He, D.; Bligh, M. W.; Waite, T. D. Effects of Aggregate Structure on the Dissolution Kinetics of Citrate-Stabilized Silver Nanoparticles. *Environ. Sci. Technol.* **2013**, *47* (16), 9148–9156.

(54) Ebrahimzadeh, S.; Ghanbarzadeh, B.; Hamishehkar, H. Physical Properties of Carboxymethyl Cellulose Based Nano-Biocomposites with Graphene Nano-Platelets. *Int. J. Biol. Macromol.*

2016, *84*, 16–23.

(55) Roy, N.; Saha, N.; Kitano, T.; Saha, P. Novel Hydrogels of PVP-CMC and Their Swelling Effect on Viscoelastic Properties. *J. Appl. Polym. Sci.* **2010**, *117* (3), 1703–1710.

(56) Fekete, T.; Borsa, J.; Takács, E.; Wojnárovits, L. Synthesis and Characterization of Superabsorbent Hydrogels Based on Hydroxyethylcellulose and Acrylic Acid. *Carbohydr. Polym.* **2017**, *166*, 300–308.

(57) Khampieng, T.; Brikshavana, P.; Supaphol, P. Silver Nanoparticle-Embedded Poly (Vinyl Pyrrolidone) Hydrogel Dressing: Gamma-Ray Synthesis and Biological Evaluation. *J. Biomater. Sci. Polym. Ed.* **2014**, *25* (8), 826–842.

(58) Wu, C.; Mosher, B. P.; Lyons, K.; Zeng, T. Reducing Ability and Mechanism for Polyvinylpyrrolidone (PVP) in Silver Nanoparticles Synthesis. *J. Nanosci. Nanotechnol.* **2010**, *10* (4), 2342–2347.

(59) Borodko, Y.; Habas, S. E.; Koebel, M.; Yang, P.; Frei, H.; Somorjai, G. A. Probing the Interaction of Poly(Vinylpyrrolidone) with Platinum Nanocrystals by UV - Raman and FTIR. *J. Phys. Chem. B* **2006**, *110* (46), 23052–23059.

(60) Beer, C.; Foldbjerg, R.; Hayashi, Y.; Sutherland, D. S.; Autrup, H. Toxicity of Silver Nanoparticles-Nanoparticle or Silver Ion? *Toxicol. Lett.* **2012**, *208* (3), 286–292.

(61) Katsnelson, B. A.; Privalova, L. I.; Sutunkova, M. P.; Minigalieva, I. A.; Gurvich, V. B.; Shur, V. Y.; Shishkina, E. V; Makeyev, O. H.; Valamina, I. E.; Varaksin, A. N. Experimental Research into Metallic and Metal Oxide Nanoparticle Toxicity in Vivo. In *Bioactivity of Engineered Nanoparticles*; Springer, 2017; pp 259–319.

(62) Loo, C.-Y.; Young, P. M.; Lee, W.-H.; Cavaliere, R.; Whitchurch, C. B.; Rohanizadeh, R. Non-Cytotoxic Silver Nanoparticle-Polyvinyl Alcohol Hydrogels with Anti-Biofilm Activity: Designed as Coatings for Endotracheal Tube Materials. *Biofouling* **2014**, *30* (7), 773–788.

(63) Kang, K.; Lim, D.-H.; Choi, I.-H.; Kang, T.; Lee, K.; Moon, E.-Y.; Yang, Y.; Lee, M.-S.; Lim, J.-S. Vascular Tube Formation and Angiogenesis Induced by Polyvinylpyrrolidone-Coated Silver Nanoparticles. *Toxicol. Lett.* **2011**, *205* (3), 227–234.

(64) Liu, X.; Lin, T.; Fang, J.; Yao, G.; Zhao, H.; Dodson, M.; Wang, X. In Vivo Wound Healing and Antibacterial Performances of Electrospun Nanofibre Membranes. *J. Biomed. Mater. Res. - Part A* **2010**, *94* (2), 499–508.

(65) Wong, K. K. Y.; Liu, X. Silver Nanoparticles: The Real “Silver Bullet” in Clinical Medicine? *Medchemcomm* **2010**, *1* (2), 125–131.

(66) Liu, X.; Lee, P. Y.; Ho, C. M.; Lui, V. C. H.; Chen, Y.; Che, C. M.; Tam, P. K. H.; Wong, K. K. Y. Silver Nanoparticles Mediate Differential Responses in Keratinocytes and Fibroblasts during Skin Wound Healing. *ChemMedChem* **2010**, *5* (3), 468–475.

TOC GRAPHIC

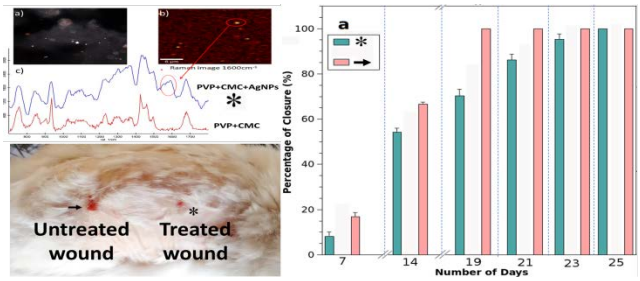
a)
b)
Raman Image 1600cm⁻¹
c)
PVP+CMC+AgNPs
PVP+CMC
Untreated wound
Treated wound

a
Percentage of Closure (%)
Number of Days
0
20
40
60
80
100
7
14
19
21
23
25